Tom Tanneberger, Sebastian Schimek, Max Kossatz, Christian Oliver Paschereit, Panagiotis Stathopoulos

Development of a swirl-stabilized H2/O2 combustion system under humidified conditions

Suggested Citation
Tanneberger, Tom; Schimek, Sebastian; Kossatz, Max; Paschereit, Christian Oliver; Stathopoulos, Panagiotis: Development of a swirl-stabilized H2/O2 combustion system under humidified conditions. - In: Digital Proceedings of the 8th European Combustion Meeting : ECM 2017. - [s.l.]: [s.n.], 2017. - ISBN: 978-953-59504-1-7, pp.1618–1623.

Development of a Swirl-Stabilized H2/O2 Combustion System under Humidified Conditions

Tom Tanneberger*, Sebastian Schimek, Max Kossatz, Christian Oliver Paschereit, Panagiotis Stathopoulos
Chair of Fluid Dynamics, Technische Universität Berlin

Abstract

The use of renewable energy sources raises the demand of fast and flexible storage techniques as well as fast power availability. A promising storage approach is the production of hydrogen and oxygen by electrolysis, which could be burned under humidified, stoichiometric conditions in a steam cycle. In this way the gases are re-electrified to provide balancing of renewable energy production or spinning network reserves. The current paper investigates the swirl-stabilized combustion of hydrogen and oxygen. The burner flow field and flame types are assessed using water tunnel PIV and OH* imaging in a combustion test rig. Parameter studies regarding the swirl intensity and thermal power are conducted.

Introduction

In order to reach the challenging commitments made at the UN Climate Change Conference 2015 in Paris [1], the emission of greenhouse gases has to be reduced significantly. On the one hand the efficiency of conventional power plants needs to be increased. On the other hand the production from renewable energy sources needs to be expanded worldwide, which raises the problem of power generation fluctuations due to the unpredictability of solar and wind energy. Technologies to balance these fluctuations will be necessary. In the short term, the kind of technologies will probably be favourable that need only small adaption to existing power plants and provide all the necessary network services simultaneously. Against this background, hydrogen, produced from an excess of renewable energy, raises more and more attention as storage medium and clean fuel.

A relative simple way of utilizing hydrogen in order to balance fluctuating energy production, is the enrichment of fossil fuels in gas turbine applications. Several projects on the combustion of hydrogen-rich fuels were initiated in the last years, for example the Advanced Hydrogen Gas Turbine Development Program by the American Department of Energy [2]. However, this technology still faces challenges and can only provide arbitrage service not contingency or frequency control. But to avoid deviations in the electricity network, some base load plants are legally bound to provide a power reserve, which can be released within a very short time. In steam power plants the method of live steam throttling is often used to provide this spinning reserve, which lowers the plants base load efficiency, leading to unnecessary emissions of greenhouse gases as well as economical loss [3]. To overcome these disadvantages, a consortium of industrial partners and research institutes in Germany developed the concept of a H_2/O_2 steam generator that burns a stoichiometric mixture of hydrogen and pure oxygen [4, 5]. The exhaust gas (superheated steam) is cooled by water to generate additional mass flow in the steam cycle for the required power boost. If hydrogen and oxygen are produced from renewable energies, this technology enables an emission free spinning reserve. The developed steam generator was adapted from rocket combustor technology and equipped with a control system to ensure a stoichiometric supply of hydrogen and oxygen. However, the exhaust steam must fulfil very challenging specifications in order to get injected in the steam cycle of a power plant: Unburned hydrogen or oxygen must be limited to a maximum of 0.01% respectively 0.03% of the exhaust flow rate to prevent corrosion or accumulation of non-condensable gases in the steam cycle [6]. In the mentioned project, an appropriate level of combustion efficiency could not be achieved with the underlying combustor design. Thus, the project ended before reaching the demonstration phase in a commercial power plant [7].

Recent developments in the field of high pressure electrolysis [8], enable the use of renewable excess energy for the production of hydrogen and oxygen under high pressure, which can directly be burned in a H_2/O_2 steam generator. Consequently, the above mentioned idea becomes attractive again and a project on stoichiometric H_2/O_2 combustion was initiated.

In the first stage of the project an experimentally proven design of a swirl-stabilized burner for humidified hydrogen/air combustion [9–11] was equipped with oxygen injectors. By changing the oxidant supply stepwise from air to pure oxygen, it was found that swirl-stabilized combustion of stoichiometric hydrogen and oxygen is feasible [12]. Based on these first results, a flexible oxy-fuel burner has been designed for further investigations. In contrast to the former H_2/O_2 steam generator project, the steam dilution is not added downstream of the a rocket flame to cool the exhaust, but the gases are directly injected into a steam environment. It is expected that the high combustion efficiency, which is common for swirl-stabilized flames due to fast mixing and exhaust recirculation, will solve the issue of unburned hydrogen and oxygen emissions. Moreover, the burner is easily scalable and thus, the steam generator can be used for both, spinning power reserves in conventional steam power plants and hydrogen re-electrification in small energy storage units. A theoretical review of methods to integrate the H_2/O_2 combustion system in existing steam cycles was already given by Schimek et al. [12].

*Corresponding author: Tom.Tanneberger@tu-berlin.de
Proceedings of the European Combustion Meeting 2017

Specific Objectives

In the present study the feasibility of steam-diluted combustion of hydrogen and oxygen is shown. To realize the concept of a stoichiometric H_2/O_2 steam generator, the burner has to feature an extremely high combustion efficiency, which can be reached by swirl stabilization. Therefore the combustor flow field needs to be optimized for a large range of operation conditions where vortex breakdown appears in the combustion chamber. This optimization is conducted isothermally using PIV in a water tunnel. The burner features flexible swirler configurations, so the flow field can be optimized according to the combustion requirements. Subsequently, the optimal configuration has to be evaluated in the combustion test rig. The degree of humidity is varied systematically to adjust the adiabatic flame temperature and record operational maps for different thermal power levels and swirler configurations. Flame shapes and exhaust temperatures are analysed and compared to the water tunnel measurements. To reach a high level of combustion efficiency, hydrogen and oxygen must burn under stoichiometric conditions. This means that the mixing quality must reach a sufficient level upstream of the flame position. Therefore, the mixing process is investigated by planar laser induced fluorescence (PLIF).

Experimental Setup

Isothermal PIV and PLIF experiments were carried out in a vertical water tunnel using a Nd:YAG laser with a wave length of 532 nm and hollow silver-coated glass spheres as seeding respectively Rhodamin 6G as dye.

For the reacting investigations, an atmospheric combustion test rig (Figure 1) was build up. A steam generator delivers a variable amount of saturated steam to a plenum upstream of the burner. Since steam is the working medium, it needs to be imposed with azimuthal momentum to generate vortex breakdown in the combustion chamber. Therefore, the steam is guided through two independently controllable swirl generators, which consist of tangential slots between the plenum and two coaxial annular ducts that channel the steam into the combustion chamber [11]. The swirl intensity of each swirl generator can be adjusted separately by blocking the tangential slots. Thus the burner has two parameters which allow a modification and optimization of the flow field. The swirler blocking for the different configurations is given in Table 1. Hydrogen and oxygen are directly injected into the combustion chamber next to the steam duct outlets. The burner is mounted to an optical accessible quartz glass combustion chamber with a diameter of 80 mm and a length of 200 mm. Downstream of the combustion chamber a water-cooled exhaust tube is placed featuring a Type S thermocouple for temperature monitoring as well as a port for sampling exhaust gas in order to analyse the combustion efficiency. An orifice at the end of the exhaust tube releases the hot gas into the atmospheric extraction unit. The flame shapes are recorded by an intensified camera with a frame rate of 125 Hz. A

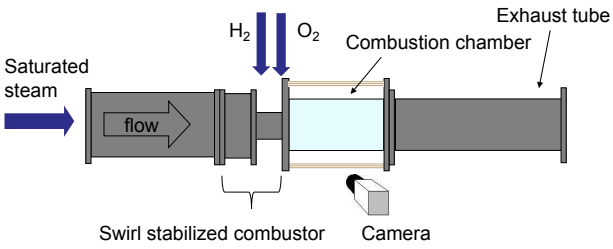

Figure 1: Combustion test rig

Configuration	inner swirler blocking %	outer swirler blocking %
I	15	25
II	40	25
III	60	25
IV	80	25
V	60	50

Table 1: Configurations

total number of 3640 images per data point were taken and averaged in the post processing. In order to cut off all light except the desired OH* chemiluminesence, the camera lens is equipped with a 307 nm band-pass filter.

Results and Discussion

As stated in the specific objectives, the combustor investigation is divided in several steps. Therefore the results are structured in the flow field, the flame shape and position, the operational maps and the mixing quality.

Flow field

At first, the combustor flow field is optimized for a large operational range. Therefore, the configurations I-IV were investigated in the water tunnel for various steam flow rates. Thereby, higher steam flow rates correspond to lower adiabatic flame temperatures (T_{ad}) in the combustion test rig. For better comparison T_{ad} is chosen as parameter for both the reacting and non-reacting tests. In Figure 2 the distance of the recirculation zone to the

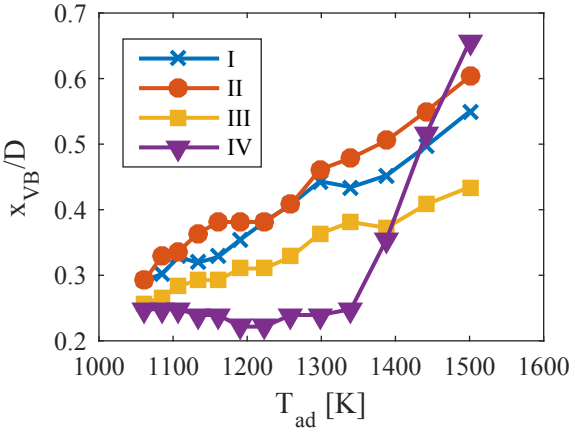

Figure 2: Distance between burner exit and recirculation zone

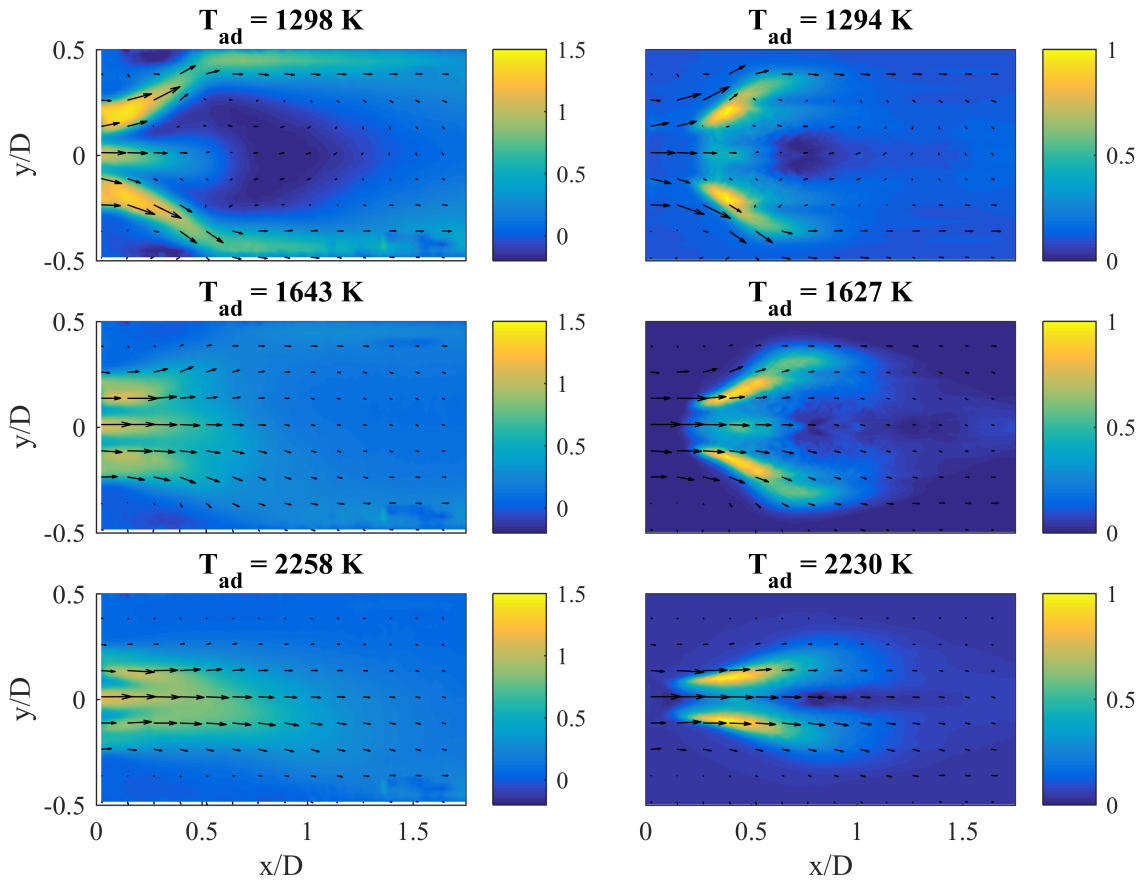

Figure 3: Normalized axial flow field from the water tunnel (l.) and normalized OH* chemiluminescence intensity (r.) of configuration III at $P = 50kW$

burner exit is plotted for the different configurations. By increasing the adiabatic flame temperature, e.g. reducing the steam dilution, the recirculation zone is shifted downstream until the tangential momentum of the steam flow is not sufficient enough to generate vortex breakdown. Thus, there is no recirculation zone present for T_{ad} being higher than 1600 K. As the swirl of the inner steam passage is intensified from Configuration I to IV, the recirculation zone is shifted closer to the burner exit. In Configuration IV the distance between burner exit and stagnation point is the smallest and constant up to $T_{ad} = 1350$ K. Afterwards the distance increases rapidly because the high pressure loss reduces the flow rate through the inner swirl passage. That's why Configuration III features the optimal ratio of swirl intensity and pressure loss to enable vortex breakdown at high adiabatic flame temperatures, respectively low steam dilution. Therefore Configuration III is further investigated in the reacting test.

Flame shape and position

According to the flow measurements, the flow field features two modes: The high swirling jet with vortex breakdown in the combustion chamber on the one hand and the stable low swirling jet on the other hand. Consequently, two different flame types, depending on the degree of steam dilution, were found for Configuration III in the combustion tests. In Figure 3, the swirl stabilized flame (upper row) and the jet flame (lower row) are depicted regarding their axial velocity field from water tunnel PIV measurements and their flame shapes from normalized OH* chemiluminescence intensity images. Both contours are superposed by two-dimensional flow vectors. At $T_{ad} = 1300$ K (upper row of Figure 3) the swirling flow underlies vortex breakdown in the combustion chamber. The axial flow is deflected towards the walls of the combustion chamber, while a recirculation zone establishes on the central axis. In its shear layers the flame is stabilized. When reducing the steam dilution the flame is shifted downstream, while getting stretched in axial and more confined in radial direction. However, even if there is no back flow present any more at $T_{ad} = 1630$ K, still a diverging of the flow can be observed due to swirling effects. This enables a stable transition from the swirl-stabilized to the jet flame type, which can be seen at $T_{ad} = 2230$ K in the last row of Figure 3. In this case, the steam and fuel streams merge to a low swirling axial jet. The flame stabilizes at the contact surface between the hydrogen and oxygen stream when sufficient mixing is reached. This type of flame has the longest stretch but lowest spreading. It is expected, that the combustion efficiency is lower for this flame shape compared to the swirl-stabilized flame, because fuel and oxidizer

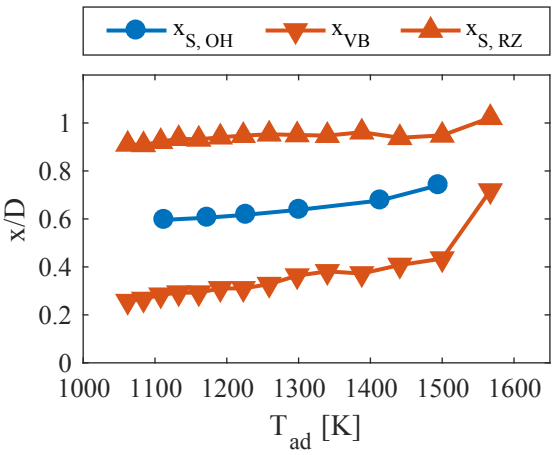

Figure 4: Distance from the burner exit to the vortex breakdown (lower line), the center of mass of the OH* chemiluminescence intensity and the center of mass of the recirculation zone (upper line) at Configuration III

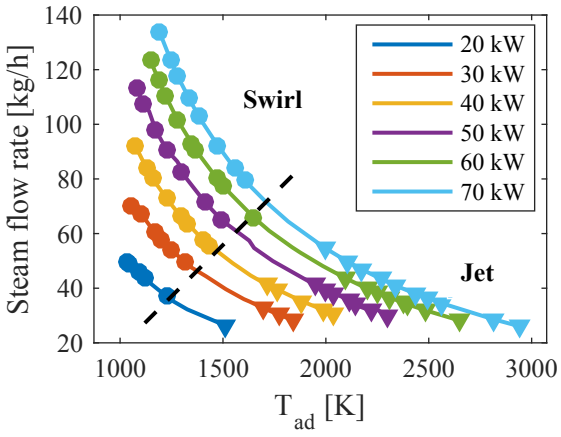

Figure 5: Operational range of Configuration III with swirl-stabilized (dot) and jet (triangle) flames

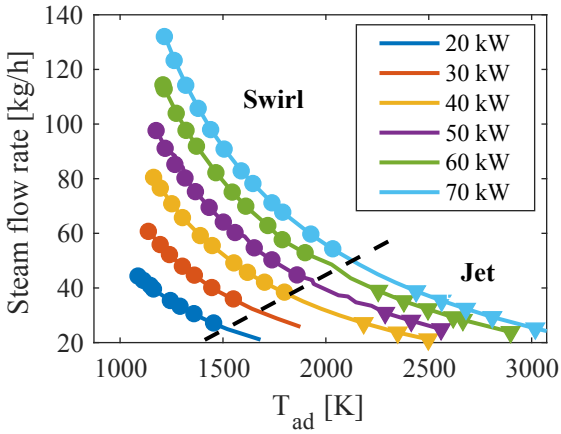

Figure 6: Operational range of Configuration V with swirl-stabilized (dot) and jet (triangle) flames

can emerge next to the flame zone. Moreover the exhaust is not recirculated, so unburned fuel can easily escape the combustion zone.

The flame shape and position depend highly on the flame type, but are only marginally influenced in the swirl-stabilized mode as pointed out in Figure 4. Even with an increase of $\Delta T_{ad} = 500\,\mathrm{K}$ the flame position, which is calculated as the center of mass of the OH* chemiluminescence intensity, varies only about $0.15\,D$. It shifts slightly downstream for increasing adiabatic flame temperatures as the recirculation zone does. The flame is located constantly at 25% of the recirculation zone for Configuration III, which indicates that the flame position depends mainly on the underlying flow field not on the chemistry. Since the time scales of the mixing process are much larger than of the reaction, the chemistry depends mainly on the mixing quality of the hydrogen and oxygen streams. Consequently, equal mixing properties lead to similar flame shapes and positions in the swirl-stabilized range. The quantification of the mixing process is discussed later on.

Operational map

In order to quantify the boundaries of the two flame types, an operational map is recorded for Configuration III with thermal powers of $P = 20 - 70\,\mathrm{kW}$. Swirl-stabilized and jet flames are marked with dots respectively triangles in Figure 5. In between them there is a slow but stable transition from one type to the other. As expected, the start of the transition increases to higher steam flow rates for higher thermal power, because P is proportional to the fuel mass flow rate. The blow off limit is nearly constant between $T_{ad} = 1050\,\mathrm{K}$ and $T_{ad} = 1200\,\mathrm{K}$. The overall operation range for swirl stabilized flames in configuration III, spreads linearly from $\Delta T_{ad} = 200\,\mathrm{K}$ at the lowest thermal power to $\Delta T_{ad} = 500\,\mathrm{K}$ at the highest. The jet flames were recorded down to a steam dilution flow rate of 26 Kg/h, which was the infrastructural limit.

As stated before, the reason for the transition to the jet flame is that the swirl intensity is not sufficient to enable vortex breakdown for low steam dilution. Since further increase of the swirl intensity in the inner steam duct is not useful (as shown in Figure 2) because of the high pressure loss, the swirling intensity of the outer steam flow has to be intensified to shift the transition towards lower steam dilution, respectively higher adiabatic flame temperatures. This is done in configuration V, where the blockage of the outer swirl generator is increased from 25% to 50%. The result is a much larger operation range for the swirl-stabilized flame as shown in Figure 6, which allows to operate the burner at higher adiabatic flame temperatures. Thus, less steam is required as diluent. In real case operation, the adiabatic flame temperature is defined by the machine boundary conditions as turbine inlet temperature and the required power output. Nevertheless, a large stability range is absolutely necessary for flexible plant operation.

In order to quantify the amount of necessary steam dilution, a steam generation factor is defined as follows:

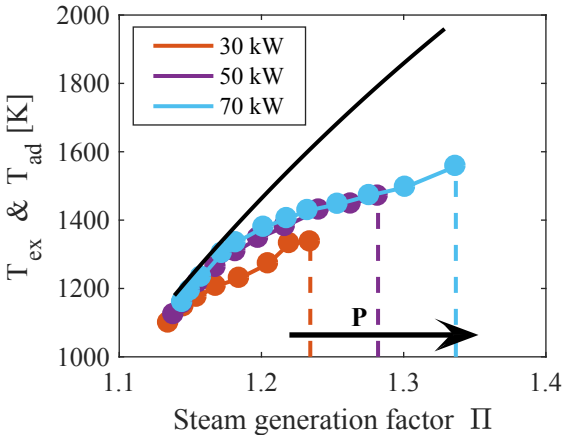

Figure 7: Adiabatic flame and exhaust (dot) temperature of Configuration V with a thermal power of 30, 50 and 70*kW*

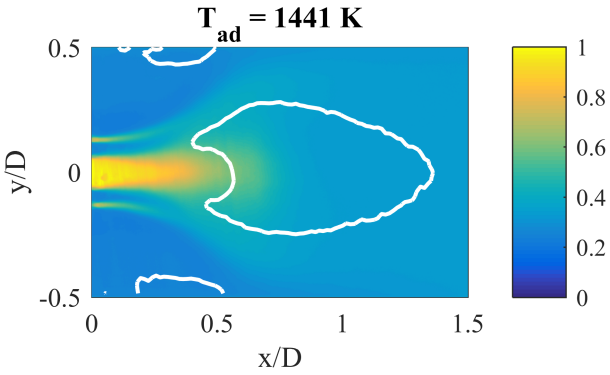

Figure 8: Normalized summed concentration of hydrogen and oxygen for Configuration I with the contour line of zero axial velocity

$$\Pi = \frac{\dot{m}_{out}}{\dot{m}_{in}} = \frac{\dot{m}_{H_2O} + \dot{m}_{H_2} + \dot{m}_{O_2}}{\dot{m}_{H_2O}}. \quad (1)$$

The steam generation factor gives the ratio of outlet steam flow rate to inlet steam flow rate. For example $\Pi = 1.3$ means that the steam generator delivers 30% of fresh steam relative to the necessary dilution. Figure 7 shows the ranges of the swirl-stabilized flames over Π for Configuration V at a thermal power of $P = 30, 50$ and 70 kW. For higher thermal power the upper limit increases. At the largest investigated power the steam generator can elevate the steam flow rate by 34%. For low steam generation rates, the measured exhaust temperature (Type S thermocouple) is close to the adiabatic flame temperature, while at higher Π the exhaust temperature increases significantly slower than the adiabatic flame temperature. This stems probably from higher heat loses due to radiation at the less diluted flame.

Mixing quality

Subsequently to the PIV measurements, mixing investigations were conducted in the water tunnel for a few data points on Configuration I and IV. Since Configuration I has also been tested in the reacting tests, it is exemplarily chosen for presenting the mixing results. The normalized concentration of hydrogen and oxygen (summed up) is shown in Figure 8, superposed by the stagnation line, e.g. the contour line of zero axial velocity. In the beginning of the combustion chamber the hydrogen injection acts like a round jet at the central axis, featuring poor mixing with the surrounding steam flow. Similar counts for the oxygen injection. Due to the occurrence of the vortex breakdown the penetration of the jet into the combustion chamber is stopped at $x/D = 0.5$. Thus the hydrogen is forced outwards into the shear layers of the recirculation zone where it mixes with the oxygen stream. The axial development of the mixing process is given by

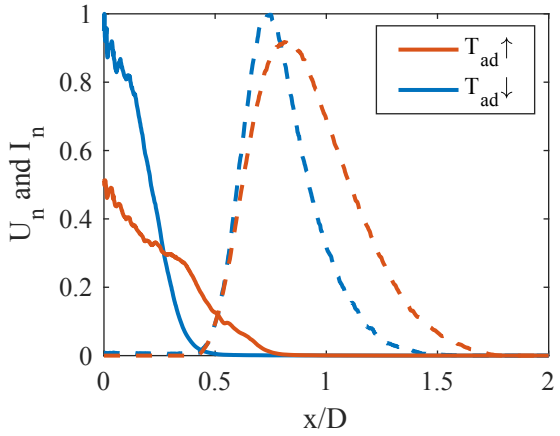

Figure 9: Normalized spatial unmixedness (-) (T_{ad} = 1072 K, 1441 K) and normalized, radial integrated OH* intensity (- -) (T_{ad} = 1175 K, 1450 K) for Configuration I

the spatial unmixedness:

$$U(x) = \frac{\langle (\overline{c(x,y)} - \langle \overline{c} \rangle)^2 \rangle}{c_\infty (1 - c_\infty)}. \quad (2)$$

Please note, that here the spatial unmixedness is not determined from cross sections (as usual), but from the axial slice in Figure 8. Accordingly, $U(x)$ gives a rather qualitative than quantitative statement. The axial trend is shown normalized in Figure 9. As stated above, the recirculation zone is shifted upstream for lower adiabatic flame temperatures respectively higher steam dilution (Figure 2). Accordingly, the hydrogen jet decays earlier which enables faster mixing. For comparison, also the flame position is indicated in Figure 9. Therefore the OH* intensity is integrated over the radius and plotted normalized for similar adiabatic flame temperatures. In both cases, e.g. high and low T_{ad}, the mixing process is finished prior to the point of maximum OH* chemiluminescence intensity. Since the flame position varies less than the mixing time, it could be expected that the equiv-

alence ratio is more homogeneous at lower T_{ad} and therefore the combustion efficiency increases. On the other hand, it had been shown before that the flame shape and position in the swirl-stabilized regime depends mainly on the flow field and less on the chemistry. Thus the mixing quality seems to sufficient in both cases. However, the combustion efficiency has to be examined in the future to proof the applicability of the H_2/O_2 steam generator.

Conclusions

The earlier idea of producing high temperature steam by the combustion of hydrogen and oxygen for power generation is revitalized in the background of today's energy production changes. While in prior research programs a rocket engine was adapted, the current project takes advantage from the high combustion efficiency of swirl-stabilized flames. In the present study first results of a fundamental investigation of a humidified, swirl-stabilized H_2/O_2 combustion system are presented. Measurements were conducted in a water tunnel and a combustion test rig. At first, the flow field properties are obtained for different swirl intensities in order to enlarge the range where vortex breakdown appears. Subsequently a selected configuration is analysed in the combustion test rig using OH* chemiluminescence. Depending on the existence of vortex breakdown, two flame types are found: a swirl-stabilized flame and a jet flame. In the swirl-stabilized regime the flame position seems to be only determined by the flow field. The operational range of the swirl type flame can be enlarged to adiabatic flame temperatures from $T_{ad} = 1200\,\mathrm{K}$ to $2000\,\mathrm{K}$ (at $P = 70\,\mathrm{kW}$) by strengthen the intensity of the outer swirl generator. Finally the mixing quality of the hydrogen and oxygen injection is investigated, which is necessary since sufficient mixing of reactant and oxidizer is crucial for the combustion efficiency. The results indicate, that in the swirl-stabilized regime the mixing process is converged prior to the flame front. Moreover, lower adiabatic flame temperatures, e.g. higher steam dilution, leads to faster mixing, which could influence the combustion efficiency. However, the actual combustion efficiency must be evaluated to proof the applicability of the concept regarding the requirements of unburned hydrogen and oxygen. Therefore, a similar system as introduced in [6] is currently in construction and calibration.

Acknowledgements

The research leading to this results has received funding from the European Research Council under the EU Framework Programme for Research and Innovation Horizon 2020 (grant agreement number: 641415 - BlueStep - ERC-2014-PoC).

References

[1] United Nations Framework Convention on Climate Change, Paris Agreement: UN Climate Conference, 2015.

[2] E. Bancalari, P. Chan, I. S. Diakunchak, in: 23rd International Pittsburgh Coal Conference, Pittsburgh.

[3] R. Sindelar, VGB Kraftwerkstechnik 64 Heft 7 (1984) 589–598.

[4] H. J. Sternfeld, P. Heinrich, International Journal of Hydrogen Energy 14 (1989) 703–716.

[5] H. J. Sternfeld, Acta Astronomica 37 (1995).

[6] S. Beer, O. J. Haidn, H. Willms, in: Combustion Technologies for a Clean Environment, volume 1, pp. 825–838.

[7] O. J. Haidn, D. Davidenko, I. Gökalp, in: 7th International Energy Conversion Engineering Conference.

[8] N. A. Kelly, T. L. Gibson, D. B. Ouwerkerk, International Journal of Hydrogen Energy 33 (2008) 2747–2764.

[9] T. G. Reichel, S. Terhaar, O. Paschereit, Journal of Engineering for Gas Turbines and Power 137 (2015).

[10] T. G. Reichel, K. Goeckeler, O. Paschereit, Journal of Engineering for Gas Turbines and Power 137 (2015).

[11] T. Tanneberger, T. G. Reichel, O. Krüger, S. Terhaar, C. O. Paschereit, in: Proceedings of ASME Turbo Expo 2015, ASME, 2015.

[12] S. Schimek, P. Stathopoulos, T. Tanneberger, C. O. Paschereit, in: Proceedings of ASME Turbo Expo 2015: Turbine Technical Conference and Exposition.